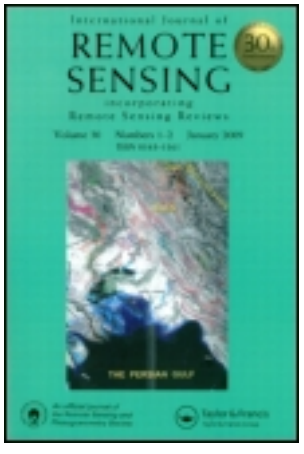

International Journal of Remote Sensing

Publication details, including instructions for authors and subscription information:
http://www.tandfonline.com/loi/tres20

Validation of MODIS-GPP product at 10 flux sites in northern China

Xufeng Wang [a b], Mingguo Ma [a], Xin Li [a], Yi Song [a b], Junlei Tan [a], Guanghui Huang [a], Zhihui Zhang [a b], Tianbao Zhao [c], Jinming Feng [c], Zhuguo Ma [c], Wei Wei [d] & Yanfen Bai [a b]

[a] Cold and Arid Regions Remote Sensing Observation System Experiment Station, Cold and Arid Regions Environmental and Engineering Research Institute, Chinese Academy of Sciences, Lanzhou, 730000, China

[b] Graduate University of Chinese Academy of Sciences, Beijing, 100049, China

[c] Key Laboratory of Regional Climate-Environment Research for the Temperate East Asia, Institute of Atmospheric Physics, Chinese Academy of Sciences, Beijing, China

[d] College of Geographical and Environmental Sciences, Northwest Normal University, Lanzhou, 730070, China

Version of record first published: 13 Sep 2012.

To cite this article: Xufeng Wang, Mingguo Ma, Xin Li, Yi Song, Junlei Tan, Guanghui Huang, Zhihui Zhang, Tianbao Zhao, Jinming Feng, Zhuguo Ma, Wei Wei & Yanfen Bai (2013): Validation of MODIS-GPP product at 10 flux sites in northern China, International Journal of Remote Sensing, 34:2, 587-599

To link to this article: http://dx.doi.org/10.1080/01431161.2012.715774

International Journal of Remote Sensing
Vol. 34, No. 2, 20 January 2013, 587–599

Validation of MODIS-GPP product at 10 flux sites in northern China

Xufeng Wang[a,b]*, Mingguo Ma[a], Xin Li[a], Yi Song[a,b], Junlei Tan[a], Guanghui Huang[a], Zhihui Zhang[a,b], Tianbao Zhao[c], Jinming Feng[c], Zhuguo Ma[c], Wei Wei[d], and Yanfen Bai[a,b]

[a]*Cold and Arid Regions Remote Sensing Observation System Experiment Station, Cold and Arid Regions Environmental and Engineering Research Institute, Chinese Academy of Sciences, Lanzhou 730000, China;* [b]*Graduate University of Chinese Academy of Sciences, Beijing 100049, China;* [c]*Key Laboratory of Regional Climate-Environment Research for the Temperate East Asia, Institute of Atmospheric Physics, Chinese Academy of Sciences, Beijing, China;* [d]*College of Geographical and Environmental Sciences, Northwest Normal University, Lanzhou 730070, China*

(*Received 19 June 2011; accepted 23 December 2011*)

Gross primary production (GPP) is an important variable in studies of the carbon cycle and climate change. The Moderate Resolution Imaging Spectroradiometer (MODIS)-GPP product (MOD17) provides global GPP data for terrestrial ecosystems; however, it is not well validated in China. In this study, an eddy covariance (EC) system observed GPP at 10 sites in northern China and was used to validate MOD17. The results indicated that MOD17 presents a strong bias in the study region due to the meteorological data, MODIS FPAR (fraction of absorbed photosynthetically active radiation) (MOD15), and the model parameters in the MODIS-GPP algorithm, Biome Parameters Look Up Table (BPLUT). Maximum light-use efficiency (ε_0) had the strongest impact on the predicted GPP of the MODIS-GPP algorithm. After using the inputs observed *in situ* and improving parameters in the MODIS-GPP algorithm, the model could explain 85% of the EC-observed GPP of the sites, whereas the MODIS-GPP algorithm without *in situ* inputs and parameters only explained 26% of EC-observed GPP.

1. Introduction

Gross primary production (GPP) is a measurement of an ecosystem's capacity to sequester carbon. GPP is usually estimated with model-based methods because GPP is difficult to measure directly (Gilmanov et al. 2003). The GPP of an ecosystem is determined by many factors, such as soil components, climate, vegetation, and ecosystem disturbance regimes. Flux towers can be used to monitor the dynamic of carbon flux at a site. In recent years, many flux-observing networks have been built throughout the world, including AmeriFlux, CarboEurope, and ChinaFlux. However, estimating the GPP of a large region is a significant challenge due to spatial variations in vegetation and climatic conditions. Remote sensing has played an important role in providing information on spatial changes in vegetation and climatic conditions (Coops et al. 2009). GPP models based on remote sensing are widely used to estimate the GPP of a large region, and carbon flux data obtained from towers can be used to validate the performance of these models.

*Corresponding author. Email: wxfgis2002@sina.com

ISSN 0143-1161 print/ISSN 1366-5901 online

http://dx.doi.org/10.1080/01431161.2012.715774
http://www.tandfonline.com

Globally, Moderate Resolution Imaging Spectroradiometer (MODIS) GPP (MOD17) is distributed by the US National Aeronautics and Space Administration (NASA). This product was calculated using a light-use efficiency model named the MODIS-GPP algorithm (Running et al. 1999). MOD17 has been validated using tower flux data from America and Europe (Chasme et al. 2009; Coops et al. 2007, 2009; Gebremichael and Barros 2006; Plummer 2006; Turner et al. 2003, 2005, 2006; Yang et al. 2007; Zhao et al. 2005, 2006). However, the model has not been widely validated in China. Nevertheless, Zhang compared the MODIS GPP with the eddy covariance (EC)-observed GPP at an alpine meadow site on the Qinghai–Tibet Plateau and a crop site in the North China Plain and found that MODIS GPP was significantly lower than EC-observed GPP (Zhang et al. 2008). Wu also found that the MODIS-GPP product clearly underestimated the GPP of temperate grassland ecosystems located in Inner Mongolia, China (Wu et al. 2008). He validated MODIS GPP for a subtropical coniferous forest in southern China and presented the same conclusions as other researchers (He et al. 2010). In this study, flux data from 10 sites located in northern China were used to validate MODIS GPP. The study sites contain grasslands, croplands, orchard, and evergreen needleleaf forest.

The objectives of this study are as follows: (1) to assess the accuracy of MODIS GPP by comparing the results to EC-observed GPP in northern China; (2) to discuss the contribution of each MODIS-GPP algorithm input to the bias of MODIS GPP; and (3) to improve the accuracy of MODIS GPP in northern China.

2. Materials and method

2.1. MODIS data

MODIS data for the years 2008 and 2009, including MODIS FPAR (fraction of absorbed photosynthetically active radiation) (MOD15A2 collection4) and MODIS GPP (MOD17A2 collection4), were downloaded from the Ameriflux web site (http://public.ornl.gov/ameriflux/). MOD17A2 is an 8 day integrated GPP value and MOD15A2 is an 8 day composite value (Poulter and Cramer 2009). The spatial resolution is 1 km. Only values obtained from a single pixel containing the observation site were extracted. MODIS data were not filtered according to the quality control (QC) information.

2.2. Site observation data

Flux and meteorology data obtained during the plant growing season (June to September) were collected from 10 sites located in northern China. Some of the ten sites were constructed by the Watershed Airborne Telemetry Experimental Research (WATER) Project (Li et al. 2009). Figure 1 shows the location of the study sites, and the type of surface cover at each site is listed in Table 1. Photosynthetically active radiation (PAR) was calculated from the shortwave solar radiation using a coefficient of 0.45. Figures 2 and 3 show the meteorological data used in the MODIS-GPP algorithm, including vapour pressure deficit (VPD), minimum air temperature ($T_{\min}$), and PAR. In order to keep the same time window with remote-sensing data, 8 day average value (for $T_{\min}$ and VPD) and 8 day integrated value (PAR) were calculated.

Typically, four steps are performed to estimate GPP from EC-observed net ecosystem exchange (NEE) data. First, QC was performed on 10 Hz flux data, including coordinate rotation and WPL correction. Second, half-hourly flux data were excluded if the sensor variance was excessive, if rainfall occurred, or if the instrument malfunctioned.

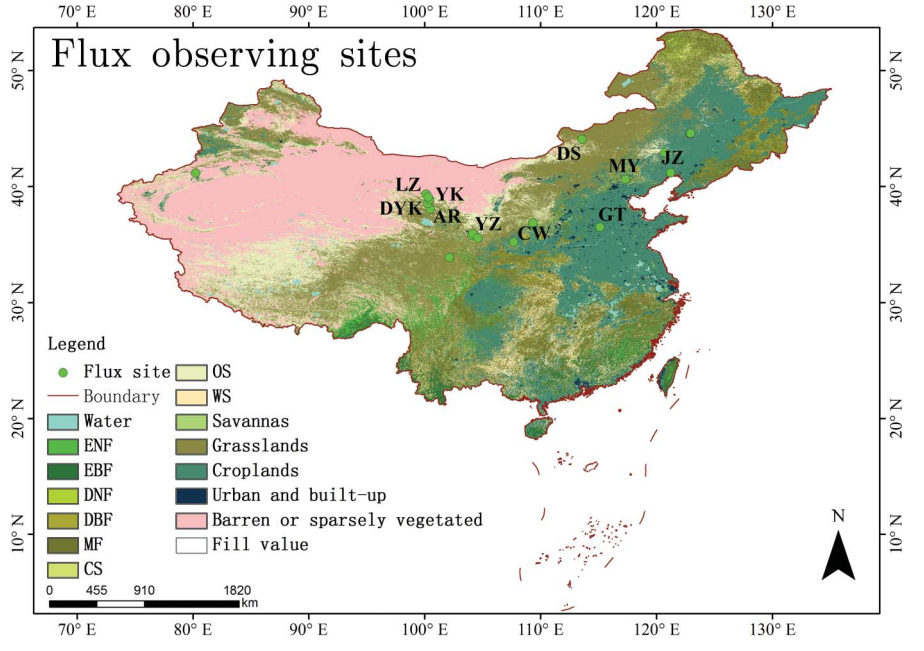

Figure 1. Map of the flux observing sites.

*AR: A'rou, CW: Changwu, DYK: Dayekou, DS: Dongsu, GT: Guantao, JZ: Jinzhou, LZ: Linze, MY: Miyun, YK: Yingke, YZ: Yuzhong. ENF: evergreen needleleaf forest, EBF: evergreen broadleaf forest, DNF: deciduous needleleaf forest, DBF: deciduous broadleaf forest, MF: mixed forest, CS: closed shrublands, OS: open shrublands, WS: woody savannas. The land-cover data are MOD12Q1 Land Cover Classification Type 2.

Table 1. Characteristics of the observation sites.

Site name	ε (grammes of carbon per MJ of APAR)		Surface type	Years for which data are available
	Calibrated*	Default		
A'rou	1.35	0.68	Grassland (Alpine meadow)	2008–2009
Changwu	0.52	0.68	Grassland	2008
Dongsu	0.69	0.68	Desert steppe	2008–2009
Dayekou	1.13	1.008	Needleleaf forest	2010
Guantao	1.82	0.68	Cropland (maize)	2009
Jingzhou	2.63	0.68	Cropland (maize)	2008–2009
Linze	2.27	0.68	Cropland (maize)	2008–2009
Miyun	1.34	1.044	Orchard (broad leaf tree)	2008–2009
Yingke	2.43	0.68	Cropland (maize)	2008–2009
Yuzhong	0.88	0.68	Grassland	2009

Note: *Calibrated ε value is calculated with APAR and EC-observed GPP during peak growing season.

During the night, the quality of NEE data was often inferior due to weak turbulent mixing at low friction velocity (u^*). Thus, night-time (defined as downward shortwave radiation <1 W m^{-2}) half-hourly flux data were excluded if the friction velocity was lower than a specific threshold. A threshold value of 0.15 m s^{-1} was used for cropland and

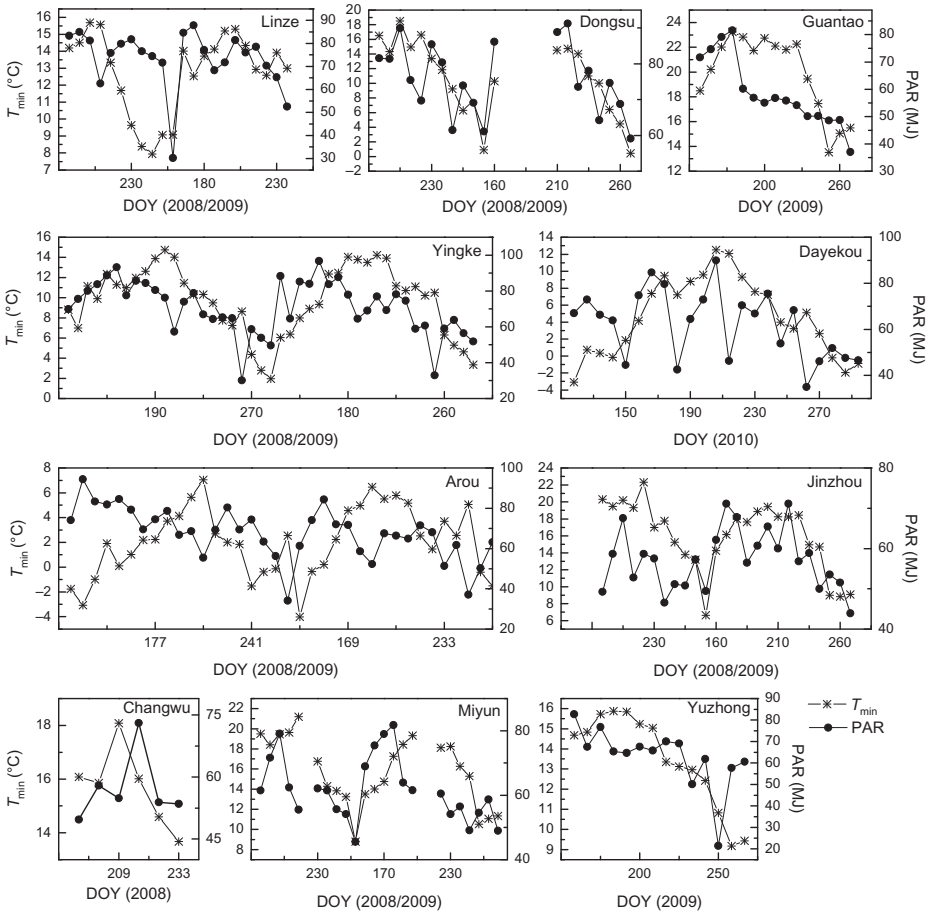

Figure 2. Plots of the 8 day average minimum daily air temperature (T_{min}) and the 8 day integrated photosynthetically active radiation (PAR) of the 10 sites. 'DOY' means 'day of year'.

grassland sites, and a threshold of 0.2 m s^{-1} was used for sites containing forests or orchards (Richardson and Hollinger 2007; Zhu et al. 2006). Third, the removed NEE value was filled according to the nonlinear relationship between flux value and environmental factors. For daytime data, the Michealis–Menten function was employed, and the Van't Hoff function was used for night-time data (Richardson and Hollinger 2007; Zhu et al. 2006). Finally, GPP can be estimated from daytime NEE and ecosystem respiration (ER). The daytime ER was calculated using the daytime soil temperature (10 cm depth) and the Van't Hoff function. Parameters of the Van't Hoff function were estimated with high-quality night-time flux data and soil temperature (Desai et al. 2008).

2.3. MODIS-GPP algorithm

MODIS GPP is calculated according to Equation (1):

$$\mathrm{GPP} = \mathrm{PAR} \times \mathrm{FPAR} \times \varepsilon_0 \times f(T_{\min}) \times f(\mathrm{VPD}), \quad (1)$$

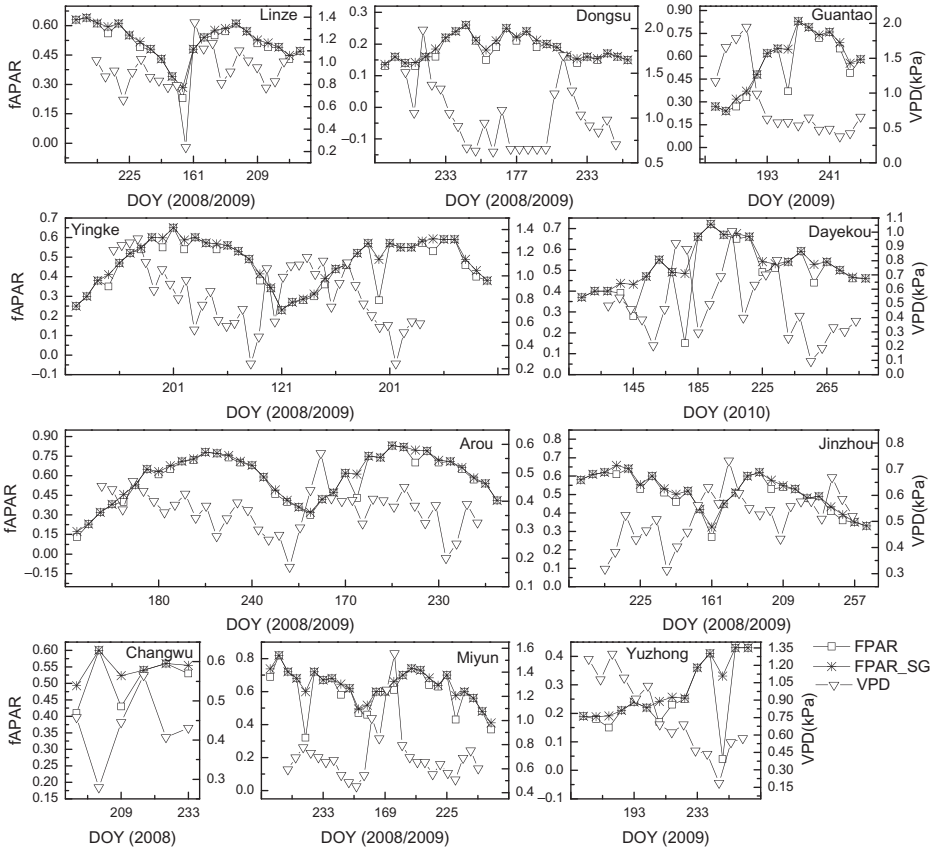

Figure 3. Plots of the FPAR (FPAR), reconstructed FPAR (FPAR_SG), and VPD of the 10 sites.

where GPP (measured in grammes of carbon per square metre per day: g C m^{-2} day^{-1}) is the gross primary production, PAR (measured in MJ) is the photosynthetically active radiation, FPAR is the fraction of absorbed photosynthetically active radiation, ε_0 (measured in grammes of carbon per MJ of absorbed photosynthetical active radiation (APAR)) is the maximum light-use efficiency, $T_{\min}$ (measured in °C) is the minimum daily temperature, and VPD [Pa] is the average vapour pressure deficit. $f(T_{\min})$ and $f(\mathrm{VPD})$ are defined as follows:

$$f(T_{\min}) = \begin{cases} 0, & T_{\min} < T_{\min_{\min}} \\ \dfrac{T_{\min} - T_{\min_{\min}}}{T_{\min_{\max}} - T_{\min_{\min}}}, & T_{\min_{\min}} < T_{\min} < T_{\min_{\max}} \\ 1, & T_{\min} > T_{\min_{\max}} \end{cases}, \tag{2}$$

$$f(\mathrm{VPD}) = \begin{cases} 0, & (\mathrm{VPD}) > (\mathrm{VPD})_{\max} \\ \dfrac{(\mathrm{VPD})_{\max} - (\mathrm{VPD})}{(\mathrm{VPD})_{\max} - (\mathrm{VPD})_{\min}}, & (\mathrm{VPD})_{\min} < (\mathrm{VPD}) < (\mathrm{VPD})_{\max} \\ 1, & (\mathrm{VPD}) < (\mathrm{VPD})_{\min} \end{cases}, \tag{3}$$

where $T_{\min_{\min}}$, $T_{\min_{\max}}$, $\mathrm{VPD}_{\max}$, and $\mathrm{VPD}_{\min}$ are species-specific parameters which can be obtained from the Biome Parameters Look Up Table (BPLUT) according to the vegetation code. The MOD17 algorithm uses the land-cover classification scheme produced by the University of Maryland (UMD) (MOD12Q1 Land Cover Classification Type 2) (Heinsch et al. 2002; Heinsch et al. 2006).

Three types of simulations were designed to analyse the uncertainty of each input in the MODIS-GPP algorithm. Sim1, site-observed meteorological data (PAR, VPD, and $T_{\min}$) and the default values of other parameters (ε_0, $T_{\min_{\min}}$, $T_{\min_{\max}}$, $\mathrm{VPD}_{\max}$, and $\mathrm{VPD}_{\min}$) were used to drive the model. Sim2, local-observed meteorological data and calibrated ε_0 were used to calculate the GPP; however, the other parameters ($T_{\min_{\min}}$, $T_{\min_{\max}}$, $\mathrm{VPD}_{\max}$, and $\mathrm{VPD}_{\min}$) were not altered. Sim3, in order to reduce the impact of the error in MODIS FPAR on the predicted GPP, smoothed FPAR using the time-series reconstructing method, locally observed meteorological data, and calibrated ε_0 were used to drive the MODIS-GPP algorithm.

For the other parameters ($T_{\min_{\max}}$, $T_{\min_{\min}}$, $\mathrm{VPD}_{\max}$, and $\mathrm{VPD}_{\min}$), the default values in BPLUT were used for all three simulations.

2.4. Reconstruction of the FPAR

The FPAR of the canopy changes slowly throughout the year due to changes in the LAI; thus, the temporal profile of FPAR should be smooth. However, due to the effects of clouds and aerosols, FPAR obtained from remote-sensing data can change abruptly, which alters the MODIS FPAR. To correct inferior values in MODIS FPAR, a time-series reconstructing algorithm named the Savizky–Golay filter was applied to FPAR time-series data. The Savizky–Golay filter can be expressed by the following equation:

$$Y_i^* = \frac{1}{2m+1} \sum_{j=-m}^{j=m} C_j Y_{i+j}, \tag{4}$$

where Y is the original time-series data, Y_i^* is the reconstructed time-series data, C_j is the jth weight of the filter window, and $2m + 1$ is the size of the filter window. The window size and order of the polynomial in the Savizky–Golay filter were set to 13 and 4 in this study, respectively (Li, Xie, and Ma 2010; Ma and Veroustraete 2006).

3. Results

3.1. MODIS GPP

MODIS GPP (GPP_MOD) was calculated with meteorological data (PAR, VPD, and Tmin) obtained from NASA's Data Assimilation Office (DAO), MODIS-retrieved FPAR, and biome-specific parameters. A comparison of MODIS GPP and EC-observed GPP is shown in Figure 4. Except for Changwu, MODIS GPP was lower than EC-observed GPP at all of the sites, especially in cropland and forest. For all of the cropland (maize) sites in this study, MODIS GPP underestimated the data by approximately 70% compared to EC-observed GPP. The lowest relative error (RE) was obtained at Changwu, where a value of 38.1% was observed (see Table 2). The coefficient of determination between MODIS GPP and EC-observed GPP was equal to 0.26 (see Table 3). The linear fit produced a slope of 0.12 (see Table 3 and Figure 5).

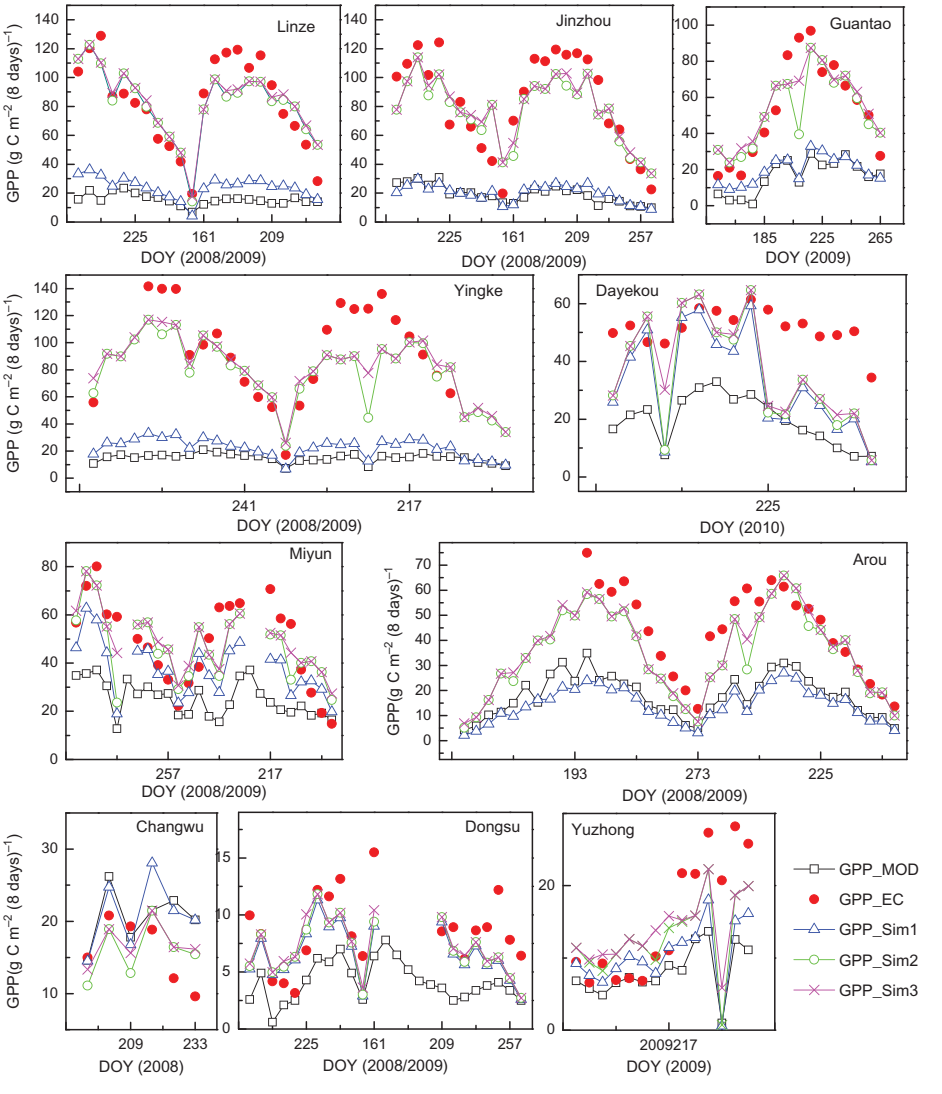

Figure 4. Plots of simulated and observed GPP at the 10 sites. GPP_MOD is the MODIS GPP; GPP_EC is the EC-observed GPP; GPP_Sim1 was calculated using the MODIS-GPP algorithm, which is driven with locally observed meteorological data (PAR, VPD, and Tmin), FPAR (MOD15A2), and other default parameters; GPP_Sim2 was calculated using calibrated ε_0 values based on GPP_Sim1; GPP_Sim3 GPP was calculated with time-series reconstructed FPAR based on GPP_Sim2.

3.2. Sim1

For Sim1, only meteorological data were replaced in the MODIS-GPP algorithm, and the other inputs and parameters were identical to those of MODIS GPP. As shown in Figure 5, the simulated GPP of the majority of sites improved slightly when tower-observed meteorological data were employed (see GPP_Sim1 in Figure 5). At all of the sites, the RE of Sim1 became lower than that of GPP_MOD. The RE changed from –54.8% to –14.5% at Dongsu and –43.3% to –14.5% at Miyun (see Table 2). The root mean square error (RMSE) of GPP_Sim1 was also improved compared to that of GPP_MOD (see Table 2).

Table 2. Statistical indices of simulated GPP and FPAR.

	MOD		Sim1		Sim2		Sim3		*r*	
	RE (%)	RMSE	RE (%)	RMSE	RE (%)	RMSE	RE (%)	RMSE	FPAR	FPAR_SG
Arou	−58.8	41.9	−66.2	31.2	−17.5	10.7	−15.6	9.2	0.68	0.75
Changwu	38.1	16.8	39.8	7.1	6.9	4.5	13.0	3.8	0.02	0.14
Dayekou	−62.9	42.0	−37.9	23.3	−32.3	22.1	−28.4	19.6	0.51	0.64
Dongsu	−54.8	8.13	−14.5	3.1	−10.7	3.0	−7.5	2.9	0.65	0.65
Guantao	−69.2	59.7	−57.9	40.0	11.5	16.6	17.8	11.5	0.72	0.87
Jinzhou	−73.5	82.5	−73.0	68.4	3.1	17.6	5.6	17.0	0.74	0.75
Linze	−78.4	87.5	−69.5	64.2	3.3	14.6	5.4	14.2	0.85	0.86
Miyun	−43.3	51.2	−14.5	17.4	6.5	14.0	11.7	11.6	0.60	0.83
Yingke	−74.1	89.4	−73.1	79.6	−5.1	25.8	−0.8	21.9	0.43	0.58
Yuzhong	−36.3	14.9	−16.5	8.3	3.2	7.2	11.2	6.3	0.66	0.93

Notes: *r* is the correlation coefficient between FPAR and observed GPP. FPAR was extracted from MOD15A2. FPAR_SG were obtained from time-series reconstructed FPAR using the Savizky–Golay filter. $\mathrm{RE} = (\sum_{i=1}^{n}(((\mathrm{SimGPP}_i - \mathrm{ObsGPP}_i)/\mathrm{ObsGPP}_i))/n) \times 100$ and $\mathrm{RMSE} = \sqrt{(1/n)\sum_{i=1}^{n}(\mathrm{SimGPP}_i - \mathrm{ObsGPP}_i)^2}$. $\mathrm{GPP}_{\mathrm{Sim},i}$ is the simulated GPP; $\mathrm{GPP}_{\mathrm{Obs},i}$ is the observed GPP; and *n* is the number of observations.

Table 3. Parameters of the linear fit between simulated and observed GPP.

	GPP_MOD	GPP_Sim1	GPP_Sim2	GPP_Sim3
Slope	0.12	0.17	0.79	0.81
Intercept	9.3	11.4	6.2	6.8
R^2	0.26	0.27	0.81	0.85

Note: R^2 is the coefficient of determination.

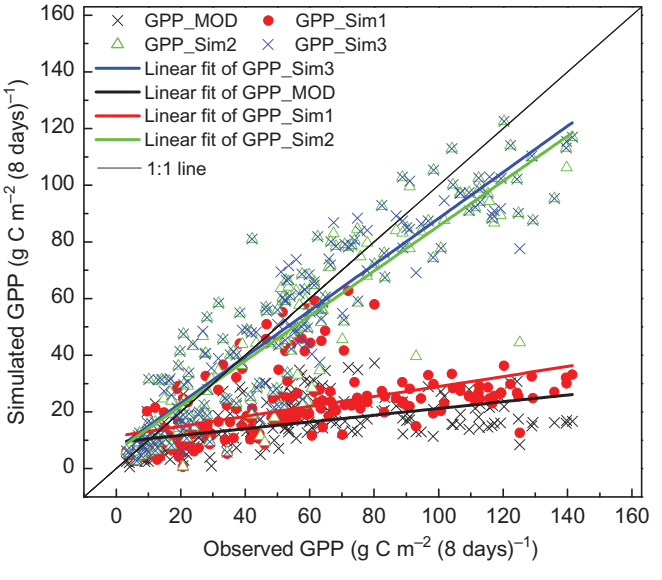

Figure 5. Scatter plot of simulated and observed GPP.

The determination coefficient between GPP_Sim1 and EC-observed GPP was equal to 0.27 (see Table 3). The linear fit between GPP_Sim1 and EC-observed GPP produced a slope of 0.17 (see Table 3 and Figure 5). Compared to GPP_MOD, both of the two statistical indices of GPP_Sim1 were superior.

3.3. Sim2

In Sim2, ε_0 was calibrated with EC-observed GPP and APAR obtained from late June to early July (see Table 1). The calibrated ε_0 values were close to the MODIS-GPP algorithm default values at only four sites. At the rest of the sites, the calibrated ε_0 values were greater than the default values. Using calibrated ε_0 values and the inputs and parameters used in Sim1, the GPP predicted by the MODIS-GPP algorithm (GPP_Sim2) was greatly improved at all of the sites. The RE of GPP_Sim2 was less than 10% at the majority of sites, and the RMSE of GPP_Sim2 was significantly lower than that of GPP_Sim1 (see Table 2). The determination coefficient between GPP_Sim2 and EC-observed GPP was equal to 0.81 (see Table 3). The linear fit between GPP_Sim2 and EC-observed GPP produced a slope of 0.79 (see Table 3 and Figure 5). Both of the statistical indices of GPP_Sim2 were greatly improved compared to that of GPP_Sim1.

3.4. Sim3

To reduce the impact of noise in MODIS FPAR on the predicted GPP, time-series MODIS FPAR was reconstructed. As shown in Figure 3, the noise of the FPAR was adjusted, and the reconstructed FPAR (FPAR_SG) had a larger correlation coefficient with EC-observed GPP than that of MODIS FPAR (FPAR) (see Table 2). Using Sim2, FPAR was replaced by FPAR_SG to calculate the GPP (GPP_Sim3). The statistical indices of GPP_Sim3 are shown in Tables 2 and 3. At all of the sites, the RMSE of GPP_Sim3 was improved compared to that of GPP_Sim2 (see Table 2). The determination coefficient between GPP_Sim3 and EC-observed GPP was equal to 0.85. The slope of the linear fit between the predicted GPP and EC-observed GPP changed from 0.79 in Sim2 to 0.81 in Sim3 (see Table 3 and Figure 5). Compared to GPP_Sim2, the RE of GPP_Sim3 decreased. Based on the RE values, GPP_Sim3 was superior to GPP_Sim2 at all of the sites.

4. Conclusions and discussion

In this study, MODIS GPP was validated, and the accuracy of the method was verified using EC-observed GPP obtained from 10 sites located in northern China. Based on the results of this study, the following conclusions can be made:

(1) The standard MODIS-GPP product displays a strong bias in the study area due to the model parameters of the MODIS-GPP algorithm BPLUT, meteorological inputs, and MODIS FPAR.
(2) The bias in the standard MODIS-GPP product mainly resulted from erroneous ε_0 values in the MODIS-GPP algorithm, BPLUT. Other inputs and parameters had smaller effects on the predicted GPP of the MODIS-GPP algorithm.
(3) Among the sites in this study, the GPP of cropland is the highest, followed by forest. The GPP of grassland is the lowest. Those sites that have data in both the years 2008 and 2009 were chosen to analyse the yearly change of GPP. The average

GPP is 141.19 g C m^{-2} (8 days)$^{-1}$ in 2008 and 135.93 g C m^{-2} (8 days)$^{-1}$ in 2009. This shows a slight decrease of GPP in northern China from 2008 to 2009.

In general, the standard MODIS GPP correctly captured the seasonal dynamics of GPP at all of the sites; however, a significant difference in the magnitude of standard MODIS GPP and EC-observed GPP was observed. At highly productive sites, the GPP was markedly underestimated by MODIS. On the contrary, at sites with low productivity, such as Changwu and Yuzhong, the MODIS GPP was close to the EC-observed GPP. This result is consistent with those obtained by Turner et al. (2006). Coops also found that standard MODIS GPP was 30% lower than EC-observed GPP (Coops et al. 2007). The observed difference in the magnitude of GPP can be attributed to three aspects, biome-specific parameters used in the MODIS-GPP algorithm, meteorological input data, and FPAR. In previous studies, the predicted global GPP changed greatly (>20 Pg C $year^{-1}$) when different meteorological data (DAO, NCEP, and ECMWF) were used to drive the MODIS-GPP algorithm (Zhao, Running, and Nemani 2006). In other words, significant uncertainties are present in the meteorological input data of standard MODIS GPP. In this study, ε_0 had the greatest impact on the predicted GPP of the MODIS-GPP algorithm, followed by FPAR. In contrast, meteorological input data had the smallest effect. The use of tower-observed meteorological data and time-series reconstructed FPAR slightly improved the GPP of MODIS-GPP algorithm; however, adjustments to ε_0 greatly improved the results. Erroneous ε_0 values produce systematically biased results. For instance, maize is a C4 plant that has greater light-use efficiency than C3 plants, and the value of ε_0 for maize cropland was approximately three times greater than the default value in the MODIS-GPP algorithm. Similarly, Zhang found that the ε_0 of wheat, a C3 plant, was approximately 1.18 g C MJ^{-1}, which is significantly higher than the MODIS-GPP algorithm default value (0.68 g C MJ^{-1}) (Zhang et al. 2008). The value of ε_0 is underestimated in standard MODIS GPP, and C4 and C3 plants are not distinguished in the MODIS-GPP algorithm. As a result, significant bias is observed in sites containing cropland, which represent 14.7% of the total land area in China (Liu et al. 2005). Noises in other parameters were also observed. Although FPAR_SG, tower meteorological data, and calibrated ε_0 values were used to drive the MODIS-GPP algorithm, significant bias was obtained in Dayekou, which presented an RE of –28%. After $T_{\mathrm{min}_{\mathrm{min}}}$ and $T_{\mathrm{min}_{\mathrm{max}}}$ were adjusted from the default values of −8°C and 8.31°C to −12°C and 5°C, the RE at Dayekou was equal to –20%. Two methods can be used to improve the accuracy of the MODIS-GPP algorithm in the study area. First, parameters in the MODIS-GPP algorithm should be calibrated for the area, and noise in FPAR data must be removed. Second, more biome types should be introduced into the MODIS-GPP algorithm, BPLUT, because croplands such as maize and wheat have significantly different parameters. Moreover, in the grassland biome, alpine meadow and desert steppe also have different parameters.

In the last paragraphs, error from the MODIS-GPP algorithm is discussed, but there is also uncertainty in EC GPP estimation. Using different NEE partition methods will result in different GPP amounts at the same site. In this study, daytime respiration was estimated with the Van't Hoff function (night-time-based method: GPP_NB). With this method, the result may be affected by suppression of turbulence and dominance of advective fluxes at night (Lasslop et al. 2010). The light response function (daytime-based method: GPP_DB) is also a widely used partitioning method (Gilmanov et al. 2007; Lasslop et al. 2010). GPP estimated with the rectangular hyperbolic light response function (without consideration of temperature and VPD) is close to the night-time-based method (see Figure 6), and the maximal relative error is 8.8% ((GPP_NB minus GPP_DB) divided by GPP_NB).

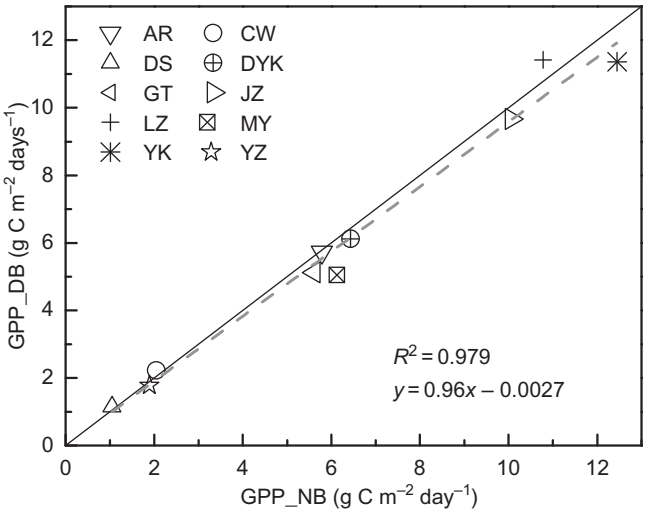

Figure 6. Scatter plot of GPP estimated with the light response function-based method (GPP_DB) and Van't Hoff function-based method (GPP_NB) with EC-observed NEE data. (AR: A'rou, CW: Changwu, DS: Dongsu, DYK: Dayekou, GT: Guantao, JZ: Jinzhou, LZ: Linze, MY: Miyun, YK: Yingke, YZ: Yuzhong.)

MODIS GPP can be used to determine the GPP within a pixel (an area of 1 km^2 in this study); however, EC measures GPP over a footprint that changes according to the wind speed and wind direction in one year. Differences in the spatial scales of the two methods may lead to differences in the predicted GPP of the MODIS-GPP algorithm and EC. Uncertainties in EC-observed GPP are also common. To obtain 8 day integrated GPP values, small gaps in the NEE data of EC must be filled, and the daytime respiration rate must be estimated. These steps also produce errors in the EC-observed GPP.

Acknowledgements

This work was supported by the National High-tech Programme (863) of China (grant number: 2009AA122104), the Chinese State Key Basic Research Project (grant number: 2009CB421305), and the National Natural Science Foundation of China (grant number: 40901095). Flux and meteorological data were provided by Coordinated Observations and Integrated Research over Arid and Semi-arid China (COIRAS) (led by the Key Laboratory of Regional Climate-Environment Research for Temperate East Asia (REC-TEA)).

References

Chasme, L., A. Barr, C. Hopkinson, H. McCaughey, P. Treitz, A. Black, and A. Shashkov. 2009. "Scaling and Assessment of GPP from MODIS Using a Combination of Airborne Lidar and Eddy Covariance Measurements Over Jack Pine Forests." *Remote Sensing of Environment* 113: 82–93.

Coops, N. C., T. A. Black, R. S. Jassal, J. A. Trofymow, and K. Morgenstern. 2007. "Comparison of MODIS, Eddy Covariance Determined and Physiologically Modelled Gross Primary Production (GPP) in a Douglas-Fir Forest Stand." *Remote Sensing of Environment* 107: 385–401.

Coops, N. C., C. J. Ferster, R. H. Waring, and J. Nightingale. 2009. "Comparison of Three Models for Predicting Gross Primary Production Across and within Forested Ecoregions in the Contiguous United States." *Remote Sensing of Environment* 113: 680–90.

Desai, A. R., A. D. Richardson, A. M. Moffat, J. Kattge, D. Y. Hollinger, A. Barr, E. Falge, A. Noormets, D. Papale, M. Reichstein, V. J. Stauch. 2008. "Cross-Site Evaluation of Eddy Covariance GPP and RE Decomposition Techniques." *Agricultural and Forest Meteorology* 148: 821–38.

Gebremichael, M., and A. P. Barros. 2006. "Evaluation of MODIS Gross Primary Productivity (GPP) in Tropical Monsoon Regions." *Remote Sensing of Environment* 100: 150–66.

Gilmanov, T. G., J. F. Soussana, L. Aires, V. Allard, C. Ammann, M. Balzarolo, Z. Barcza, C. Bernhofer, C. L. Campbell, A. Cernusca, A. Cescatti, J. Clifton-Brown, B. O. M. Dirks, S. Dore, W. Eugster, J. Fuhrer, C. Gimeno, T. Gruenwald, L. Haszpra, A. Hensen, A. Ibrom, A. F. G. Jacobs, M. B. Jones, G. Lanigan, T. Laurila, A. Lohila, G. Manca, B. Marcolla, Z. Nagy, K. Pilegaard, K. Pinter, C. Pio, A. Raschi, N. Rogiers, M. J. Sanz, P. Stefani, M. Sutton, Z. Tuba, R. Valentini, M. L. Williams, G. Wohlfahrt. 2007. "Partitionning European Grassland Net Ecosystem CO_2 Exchange into Gross Primary Productivity and Ecosystem Respiration Using Light Response Function Analysis." *Agriculture, Ecosystem and Environment* 121: 93–120.

Gilmanov, T. G., S. B. Verma, P. L. Sims, T. P. Meyers, J. A. Bradford, G. G. Burba, and A. E. Suyker. 2003. "Gross Primary Production and Light Response Parameters of Four Southern Plains Ecosystems Estimated Using Long-Term CO2-Flux Tower Measurements." *Global Biogeochemical Cycles* 17, no. 2: 1017.

He, M. Z., Y. L. Zhou, G. H. Liu, W. M. Ju, X. F. Li, and G. L. Zhu. 2010. *Validation of MODIS Gross Primary Productivity for a Subtropical Coniferous Plantation in Southern China*. 18th International Conference on Geoinformatics, Peking University, Beijing, June 18–20, 1689–93.

Heinsch, F. A., M. Reeves, P. Votava, S. Kang, C. Milesi, M. S. Zhao, J. Glassy, W. M. Jolly, R. Loehman, C. F. Bowker, J. S. Kimball, R.R. Nemani, S.W. Running. 2002. *User's Guide GPP and NPP (MOD17A2/A3) Products NASA MODIS Land Algorithm*. Version 2.0. University of Montana, SCF At-Launch algorithm ATBD Document. Accessed August 14, 2012. http://www.ntsg.umt.edu/sites/ntsg.umt.edu/files/modis/MOD17UsersGuide.pdf.

Heinsch, F. A., M. S. Zhao, S. W. Running, J. S. Kimball, R. R. Nemani, K. J. Davis, P. V. Bolstad, B. D. Cook, A. R. Desai, D. M. Ricciuto, B. E. Law, W. C. Oechel, H. Kwon, H. Y. Luo, S. C. Wofsy, A. L. Dunn, J. W. Munger, D. D. Baldocchi, L. K. Xu, D. Y. Hollinger, A. D. Richardson, P. C. Stoy, M. B. S. Siqueira, R. K. Monson, S. P. Burns, L. B. Flanagan. 2006. "Evaluation of Remote Sensing Based Terrestrial Productivity from MODIS Using Regional Tower Eddy Flux Network Observations." *IEEE Transactions on Geoscience and Remote Sensing* 44, no. 7: 1908–25.

Lasslop, G., M. Reichstein, D. Papale, A. D. Richardson, A. Arneth, A. Barr, P. Stoy, G. Wohlfahrt. 2010. "Separation of Net Ecosystem Exchange into Assimilation and Respiration Using a Light Response Curve Approach: Critical Issues and Global Evaluation." *Global Change Biology* 16: 187–208.

Li, X., X. W. Li, Z. Y. Li, M. G. Ma, J. Wang, Q. Xiao, Q. Liu, T. Che, E. X. Chen, G. J. Yan, Z. Y. Hu, L. X. Zhang, R. Z. Chu, P. X. Su, Q. H. Liu, S. M. Liu, J. D. Wang, Z. Niu, Y. Chen, R. Jin, W. Z. Wang, Y. H. Ran, X. Z. Xin, H. Z. Ren. 2009. "Watershed Allied Telemetry Experimental Research." *Journal of Geophysical Research* 114, no. D22103. doi:10.1029/2008JD011590.

Li, H. Y., Y. W. Xie, and M. G. Ma. 2010. "Reconstruction of Temporal NDVI Dataset: Evaluation and Case Study." *Remote Sensing Technology and Application* 24, no. 5: 596–602.

Liu, J. Y., M. L. Liu, H. Q. Tian, D. F. Zhuang, Z. X. Zhang, W. Zhang, X. M. Tang, X. Z. Deng. 2005. "Spatial and Temporal Patterns of China's Cropland During 1990–2000: An Analysis Based on Landsat TM Data." *Remote Sensing of Enviroment* 98: 442–56.

Ma, M. G., and F. Veroustraete. 2006. "Reconstructing Pathfinder AVHRR Land NDVI Time-Series Data for the Northwest of China." *Advances in Space Research* 37: 835–40.

Plummer, S. 2006. "On Validation of the MODIS Gross Primary Production Product." *IEEE Transactions on Geoscience and Remote Sensing* 44: 1936–38.

Poulter, B., and W. Cramer. 2009. "Satellite Remote Sensing of Tropical Forest Canopies and Their Seasonal Dynamics." *International Journal of Remote Sensing* 30, no. 24: 6575–90.

Richardson, A. D., and D. Y. Hollinger. 2007. "A Method to Estimate the Additional Uncertainty in Gap-Filled NEE Resulting from Long Gaps in the CO_2 Flux Record." *Agricultural and Forest Meteorology* 147: 199–208.

Running, S. W., R. Nemani, J. M. Glassy, and P. E. Thornton, 1999. *MODIS Daily Photosynthesis (PSN) and Annual Net Primary Production (NPP) Product (MOD17). Algorithm Theoretical Basis Document.* Version 3.0. University of Montana, SCF At-Launch algorithm ATBD Document. http://modis.gsfc.nasa.gov/data/atbd/atbd_mod16.pdf.

Turner, D. P., W. D. Ritts, W. B. Cohen, S. T. Gower, S. W. Running, M. S. Zhao, M. H. Costa, A. A. Kirschbaum, J. M. Ham, S. R. Saleska, D. E. Ahl. 2006. "Evaluation of MODIS NPP and GPP Products Across Multiple Biomes." *Remote Sensing of Environment* 102: 282–92.

Turner, D. P., W. D. Ritts, W. B. Cohen, S. T. Gower, M. S. Zhao, S. W. Running, S. C. Wofsy, S. Urbanski, A. L. Dunn, J. W. Munger. 2003. "Scaling Gross Primary Production (GPP) Over Boreal and Deciduous Forest Landscapes in Support of MODIS GPP Product Validation." *Remote Sensing of Environment* 88: 256–70.

Turner, D. P., W. D. Ritts, W. B. Cohen, T. K. Maeirsperger, S. T. Gower, A. A. Kirschbaum, A. L. Dunn, B. E. Law, J. L. Campbell, W. C. Oechel, H. J. Kwon, T. P. Meyers, E. E. Small, S. A. Kurc, J. A. Gamon. 2005. "Site-Level Evaluation of Satellite-Based Global Terrestrial Gross Primary Production and Net Primary Production Monitoring." *Global Change Biology* 11: 666–84.

Wu, W. X., S. Q. Wang, X. M. Xiao, G. R. Yu, Y. L. Fu, and Y. B. Hao. 2008. "Modeling Gross Primary Production of a Temperate Grassland Ecosystem in Inner Mongolia, China, Using MODIS Imagery and Climate Data." *Science in China Series D: Earth Sciences* 51, no. 10: 1501–12.

Yang, F. H., K. Lchii, M. A. White, H. Hashimoto, A. R. Michaelis, P. Votava, A. X. Zhu, A. Huete, S. W. Running, R. R. Nemani. 2007. "Developing a Continental-Scale Measure of Gross Primary Production by Combining MODIS and AMEriFLUX Data Through Support Vector Machine Approach." *Remote Sensing of Environment* 110: 109–22.

Zhao, M. S., F. A. Heinsch, R. R. Nemani, and S. W. Running. 2005. "Improvements of the MODIS Terrestrial Gross and Net Primary Production Global Data Set." *Remote Sensing of Environment* 95: 164–79.

Zhao, M. S., S. W. Running, and R. R. Nemani. 2006. "Sensitivity of Moderate Resolution Imaging Spectroradiometer (MODIS) Terrestrial Primary Production to the Accuracy of Meteorological Reanalyses." *Journal of Geophysical Research* 111: G01002.

Zhang, Y. Q., Q. Yu, J. Jiang, and Y. H. Tan. 2008. "Calibration of Terra/MODIS Gross Primary Production Over an Irrigated Cropland on the North China Plain and an Alpine Meadow on the Tibetan Plateau." *Global Change Biology* 14: 757–67.

Zhu, Z. L., X. M. Sun, X. F. Wen, Y. L. Zhou, J. Tian, and G. F. Yuan. 2006. "Study on the Processing Method of Nighttime CO_2 Eddy Covariance Flux Data in ChinaFLUX." *Science in China Series D: Earth Sciences* 49, no. Supp. II: 36–46.